ELSEVIER

Surface Science 493 (2001) 633–643

SURFACE SCIENCE

www.elsevier.com/locate/susc

Independently driven four-tip probes for conductivity measurements in ultrahigh vacuum

Ichiro Shiraki [a,b], Fuhito Tanabe [a], Rei Hobara [a], Tadaaki Nagao [a,c], Shuji Hasegawa [a,c,*]

[a] *Department of Physics, School of Science, University of Tokyo, 7-3-1 Hongo, Bunkyo-ku, Tokyo 113-0033, Japan*
[b] *Japan Society for the Promotion of Science, Yamato Bldg., 5-3-1 Kohjimachi, Chiyoda-ku, Tokyo 102-8471, Japan*
[c] *Core Research for Evolutional Science and Technology, The Japan Science and Technology Corporation, Kawaguchi Center Building, Hon-cho 4-1-8, Kawaguchi, Saitama 332-0012, Japan*

Received 21 September 2000; accepted for publication 28 February 2001

Abstract

To measure electrical conductivity of materials in scales ranging from nanometer to millimeter, a four-point probe system was developed and installed in an ultrahigh-vacuum scanning electron microscope (UHV-SEM). Each probe, made of a W tip, was independently driven with piezoelectric actuators and a scanner in *XYZ* directions to achieve precise positioning in nanometer scales. The SEM was used for observing the tips for positioning, as well as the sample surface together with scanning reflection-high-energy electron diffraction capability. This four-point probe system has two kinds of special devices. One is octapole tube-type scanners for tip scanning parallel to the sample surface with negligible displacements normal to the surface. Another is a pre-amplifier which can be switched in current measurement mode between tunnel contact for scanning tunneling microscopy and direct contact for four-point probe method. The electrical resistance of a silicon crystal with a Si(1 1 1)-7 × 7 clean surface was measured with this machine as a function of probe spacing between 1 mm and 1 μm. The result clearly showed an enhancement of surface sensitivity in resistance measurement by reducing the probe spacing.

Keywords: Surface electrical transport (surface conductivity, surface recombination, etc.); Scanning electron microscopy (SEM); Silicon

1. Introduction

For integrating electronic devices at nanometer scales, it is important to measure electrical properties of materials in the same scale. Especially, the electrical properties are expected to depend on atomic-level structures near surfaces of the materials such as atomic steps and domains boundaries of surface superstructures. Electrical conductivity of atomic wires and other nanometer-scale structures on surfaces is also required to be directly measured. Not only from such technological importance, but also from fundamental interest in condensed matter physics, electrical conductivity due to surface-state bands of surface superstructures was measured in situ in ultra high-vacuum

* Corresponding author. Address: Department of Physics, School of Science, University of Tokyo, 7-3-1 Hongo, Bunkyo-ku, Tokyo 113-0033, Japan. Tel./fax: +81-3-5841-4167.
E-mail address: shuji@surface.phys.s.u-tokyo.ac.jp (S. Hasegawa).

0039-6028/01/$ - see front matter
PII: S0039-6028(01)01276-6

(UHV) by conventional macroscopic four-point probe method (probe spacing being in mm order) [1], and also by microscopic four-point probe method (probe spacing being 8 μm) [2,3].

As for a Si(1 1 1)-7×7 clean surface and a Si(1 1 1)-$\sqrt{3} \times \sqrt{3}$–Ag surface, for example, the difference in surface electrical conductance between them was measured with the microscopic four-point probes; it was much larger than that measured with macroscopic four-point probes [3, 4]. This means that the sensitivity for surface conductivity is getting higher with smaller probe spacing because current leaking into the underlying bulk is reduced with the probe spacing [2,4,5]. Furthermore it is expected that the measured surface conductivity can be getting intrinsic ones if the probe spacing is on the order of nanometer because carrier scattering by surface defects can be avoided by selecting the surface areas to be measured. If nm-spacing probes are available, local surface-state conductivity in a single domain and the influence of surface defects can be directly measured.

Several groups have already developed machines with independently driven double tips for such purposes. One of the machines was constructed by Aono et al. [6]. They successfully made the W-tip probes to approach to close each other in ≈100 nm on a sample surface. In the measurement of surface conductivity with the two-point probe

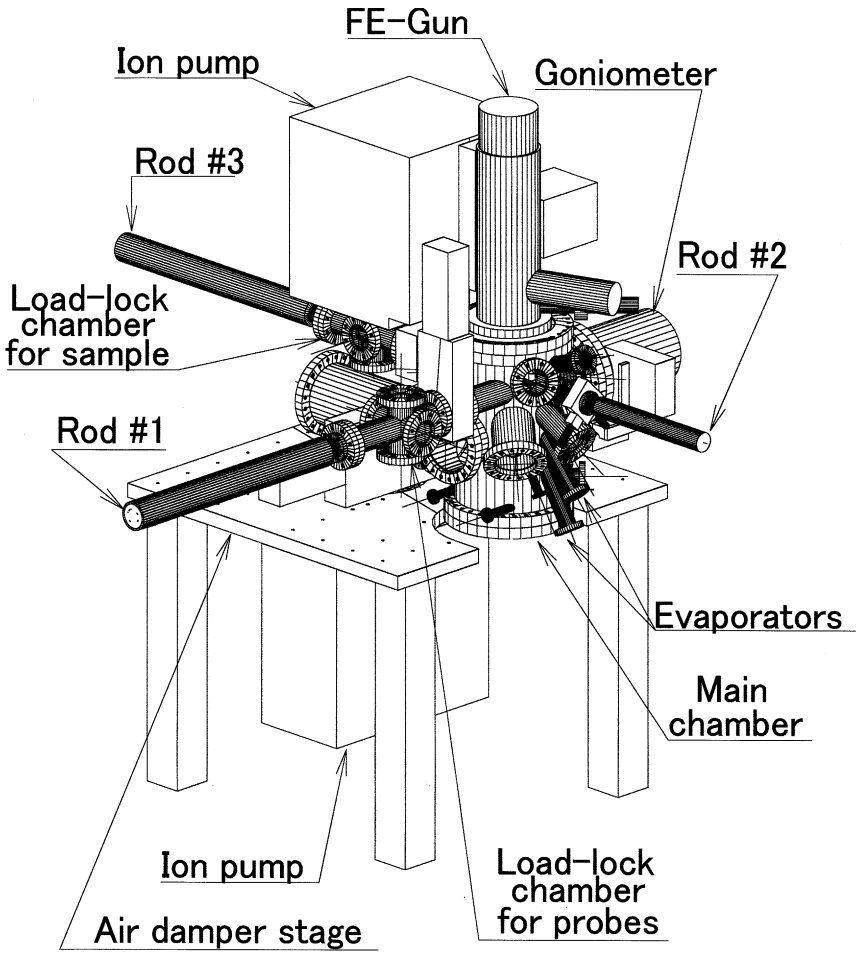

Fig. 1. Overview of the independently driven four-tip probe system combined with UHV-SEM-SREM-RHEED.

method, however, it is necessary to estimate the influence of contact resistances between the probes and sample surface, which is practically very difficult in many cases because the contact resistance is much higher than the surface resistance to be measured and sensitively depends on the contact conditions. For these reasons, it is necessary to develop four-point probes with variable probe spacing at nanometer scales in UHV, in which the contact resistance matters little basically. Moreover, such a probe system should be combined with an ability of imaging the sample surface to select the area to be measured as well as to observe the probes themselves for positioning. We have constructed such a four-point probe system with independently driven four W tips, each probe of which has capability for scanning tunneling microscope (STM) in UHV. The positioning of each probe can be done in situ with aid of SEM. The four probes can be used for four-point probe measurements of conductivity. In this paper, we describe the details of the apparatus and a demonstration of the probe positioning, together with resistance data of a Si(1 1 1)-7×7 clean crystal measured with this apparatus by a linear four-point probe method as a function of the probe spacing.

2. Instrument

2.1. Overview and components

Fig. 1 shows an overview of the instrument, which consists of three chambers, a main chamber and two load-lock chambers for introducing probes and samples from atmosphere to UHV. On top of the main chamber, a cold-cathode field-emission (FE) electron gun is attached for SEM, which enables also reflection-high-energy electron diffraction (RHEED) and scanning reflection electron

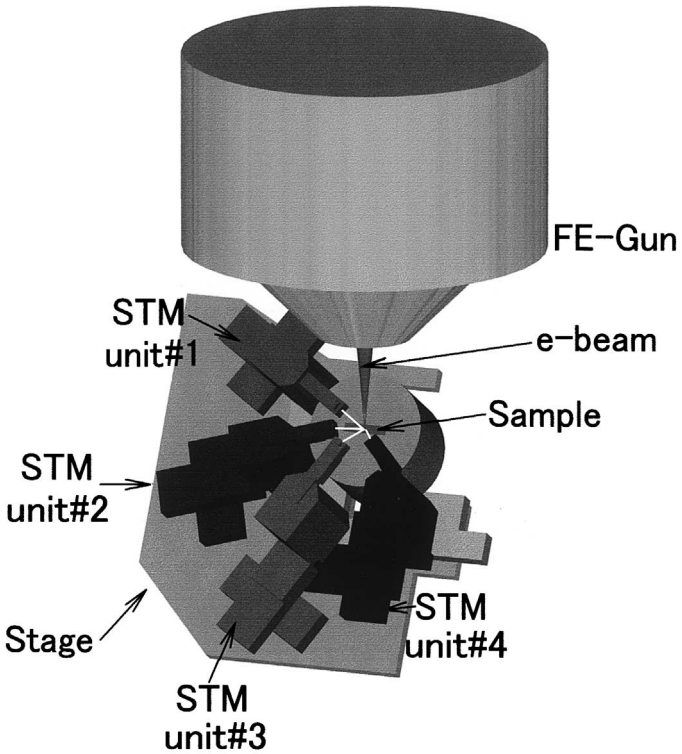

Fig. 2. The arrangement of four sets of tip actuators (STM units) and SEM electron beam around the sample.

microscopy (SREM) observations of the sample surfaces. A side-entry goniometer is installed in the main chamber, and it has a goniometer stage on which four sets of probe actuators and scanners are mounted together with a rotatory sample holder. There are two evaporators in the main chamber. All of these components are mounted on an air damper stage for isolation from environmental vibration. Thus, surface cleaning by direct-current heating, deposition of metals, preparation and confirmation of surface structures, and electrical resistance measurements can be done in situ. All of the chambers and assembled parts were designed by Design CAD 2D/3D (MATSUBO).

Fig. 2 shows the arrangement around the sample, with the FE electron column and the four sets of the probe actuators (STM units) mounted on the goniometer stage. Its photograph is shown in

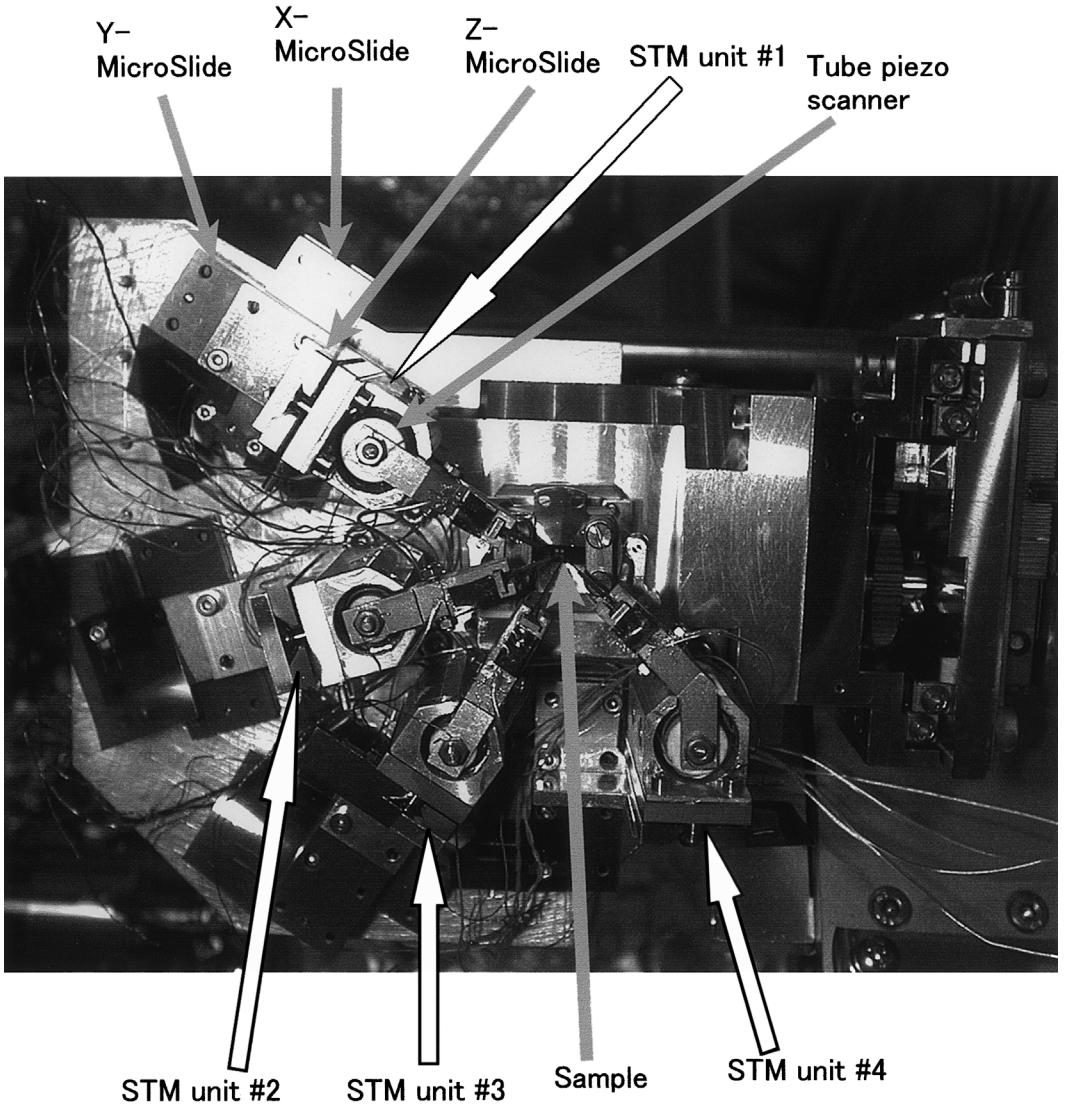

Fig. 3. A photograph of the goniometer stage with four sets of STM units.

Fig. 3. The four STM units surround the sample, and they are driven independently. The whole stage can be moved by the goniometer in *XYZ* directions (20 mm travel distance in each direction) and be tilted (0–90°) with respect to the incident electron beam, which is necessary for grazing-incidence SEM and RHEED-SREM. The sample holder can be azimuthally rotated (0–360°) with respect to the STM units to select the azimuth angle of the incident electron beam.

The rod no. 3 shown in Fig. 1 is for transferring the sample holder, for which the stage is made in horizontal by the goniometer, that is, the tilt angle of the stage is 0°. The rod no. 2 in Fig. 1 is for transferring the probe tips, for which the stage is made in vertical (the tilt angle is 90°). On the end of the rod no. 1, the parking unit for the probes is attached, on which six probes with holders can be loaded at one time. The probes can be heated in UHV by forcing electrical current between the probe and a Ta wire contacting to it. Additionally, high voltages can be applied between the probes and GND, with which Fowler–Nordheim plots can be taken to estimate the curvature of probes. The heating and the high voltage application can be done simultaneously.

2.2. Probe actuators and scanners

Fig. 4 shows one of the STM units (probe actuators), which consists of three sets of OMICRON microslides (40–400 nm movement per step in 5 mm travel distance). A tube-type piezoelectric

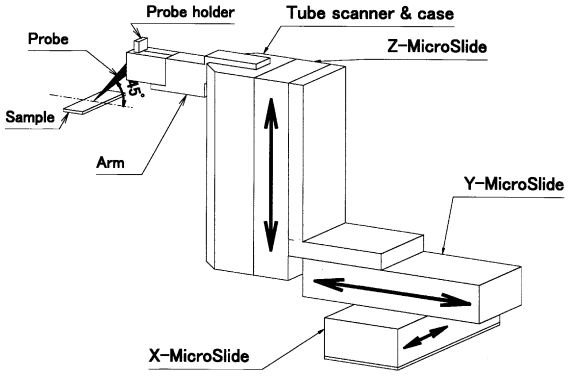

Fig. 4. A schematic view of one of the STM units.

scanner is set on the *Z*-Microslide, covered by a metal case for electric shielding. The case shields leakage field of the high voltages applied to the scanner (up to ±150 V), which prevents electrical noise in SEM-SREM observations. The Microslides and tube scanner are used for course motion and fine positioning of each probe, respectively. On top of the tube scanner, an arm is attached, on the other end of which a probe holder is mounted magnetically. The magnet is set on a ceramic block. Each probe has an angle of 45° from the surface normal of the sample so that the four probes can be brought close to each other by precise positioning. These arrangements enable measurements of electrical conductivity by four-point probe method in microscopic regions and microscopic objects.

The tube scanner is a special one that is shown in Fig. 5(b), which should be compared with a conventional tube scanner shown in Fig. 5(a). When scanning in lateral (*XY*) directions parallel to the sample surface with the conventional scanner, the displacement in *Z* direction of the tip end is negligible if the tip is on the center axis of the tube scanner. But if the end of the tip is out of the center axis as shown in Fig. 5(a), *Z*-direction shift due to bending in *X* direction is not negligible. This is caused by an inclination between the top and bottom surfaces of the tube scanner. In our present system, this problem is severe because of an arm between the tube scanner and probe. To avoid this problem, we have designed a special tube scanner as shown in Fig. 5(b). The basic idea is to connect two equivalent tube scanners in series but in an opposite direction. The two scanners should have the same piezoelectric characters and dimensions. The upper tube scanner and the lower one move in symmetrically opposite ways. The same voltages are applied to pairs of +X1 and −X2 electrodes, and −X1 and +X2 electrodes (counterelectrodes to each other), respectively, for *X*-scanning. In the same way, voltages are applied to two pairs of electrodes, +Y1 and −Y2, and −Y1 and +Y2, for *Y*-scanning. By this configuration, the top surface of the scanner is basically always in parallel to the bottom surface. Hence, the unintentional displacement in *Z*-direction caused by *X*-scanning can be avoided even if the probe is

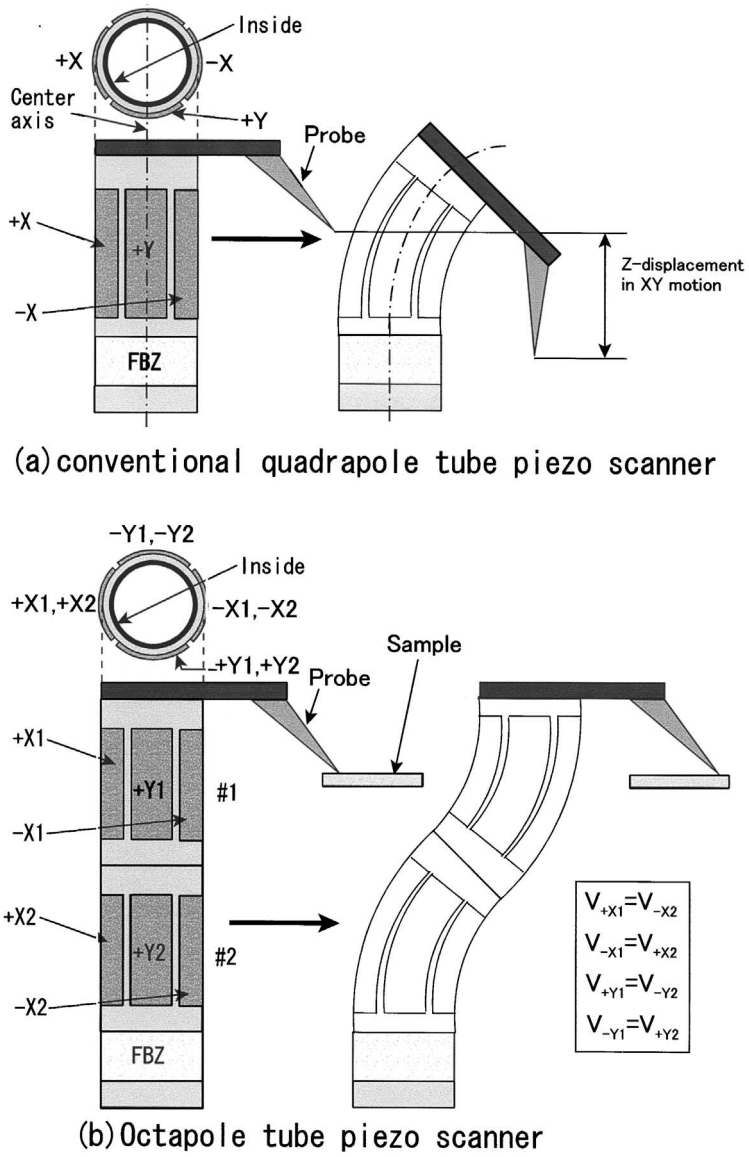

Fig. 5. Comparison between a conventional quadrapole tube-type piezoelectric scanner (a) and the newly designed octapole tube-type scanner (b).

set out of the center axis of the tube scanner. We remodeled conventional piezoelectric tube-type scanners in a way that each electrode for X and Y scanning were just separated into two parts to be X1/X2 and Y1/Y2 electrodes. With this configuration of electrodes on a scanner, its scanning ranges in XY directions are reduced to be about half of those for the conventional one.

Fig. 6 reproduces SEM images, showing the probe motion of the STM unit no. 4. Under applying 300 V to the X-direction electrodes of the tube scanner, the end of probe was moved by about 1 μm in X direction, which was about a half of the shift at a conventional quadrapole tube scanner with the same dimensions and piezoelectric characteristics. We tried to observe the Z-displacement

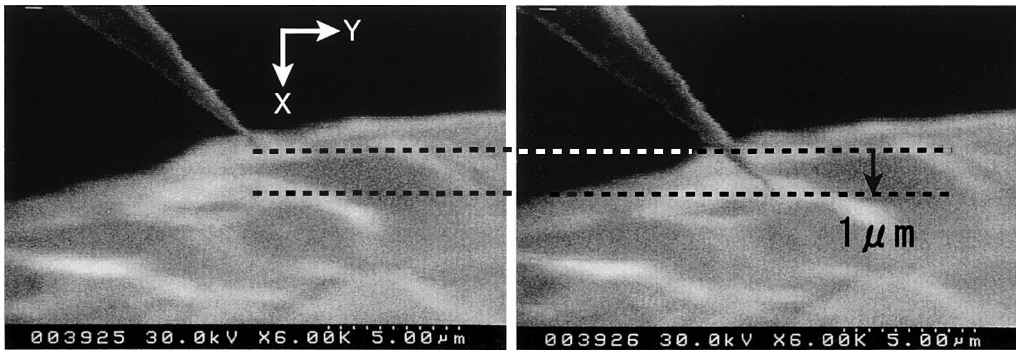

Fig. 6. Probe motion with STM unit no. 4. The probe was moved by about 1 μm in X direction (300 V applied), while the Z-displacement was not detected within the resolution of the SEM.

of the tip by SEM during this X-movement by tilting the goniometer stage by ≈90°. But we could observe no Z-displacement within the resolution of our SEM (∼10 nm). This result is an expected one from Fig. 5. Although clear STM images with atomic resolution were not yet taken with this system, the SEM images in Fig. 6 show an evidence for the newly designed octapole tube-type scanner working actually, and exhibit the possibility of application for any scanning probe microscopes.

2.3. Control system and electronics

A block diagram of the control system is shown in Fig. 7. For SEM–SREM RHEED, a controller of Hitachi S4200 system was used. SREM images were taken by selecting a diffraction spot in RHEED and by mapping its intensity in synchronizing with the scanning signal. Each STM unit was controlled by its own PC. The current lines from the four STM units were connected to a special pre-amplifier that has functions for STM I–V converter and for conductivity measurement by four-point probe method. Because it is necessary to switch the current lines when switching between the two function modes without touching the chamber and wires, some electronic switching devices should be introduced in the pre-amplifier. To switch a very low current line such as tunneling current in STM operation, leakage current at switching devices should be extremely low. For that, MAX326/7 (MAXIM) photo MOS switches were used. Their leakage current was below 1 pA at room temperature. It should be noted that the switches were used carefully because they had several hundred ohms resistance at ON condition.

Each controller for each tip consists of a PC in which some boards are mounted to control a piezoelectric-scanner driver and a Microslide controller. We chose DSP boards (TMS20C62x EVM and its daughter boards, Texas Instruments) for feedback system and digital to analog (DA)/analog to digital (AD) board for scanning signal for probes and data acquisition. In addition, a digital interface (DI) board is used for making handshakes on other PCs and the switches of the pre-amplifier that consists of four I–V converters and the measurement unit for four-point probe method. There is one master PC that monitors the function of other PCs and controls the measurements of surface conductivities by four-point probe methods. The piezo-scanner drivers are handmade, mainly composed of OP-27E, OP-227EY (Analog Devices) and 3583/4 (Burr-Brown).

3. Probe positioning

Fig. 8 demonstrates the probe positioning. The probe tips were made of W wires with electrochemical etching. First, the distances among the probes were more than 1 mm as shown in Fig. 8(a). By using microslides, the probes were positioned in

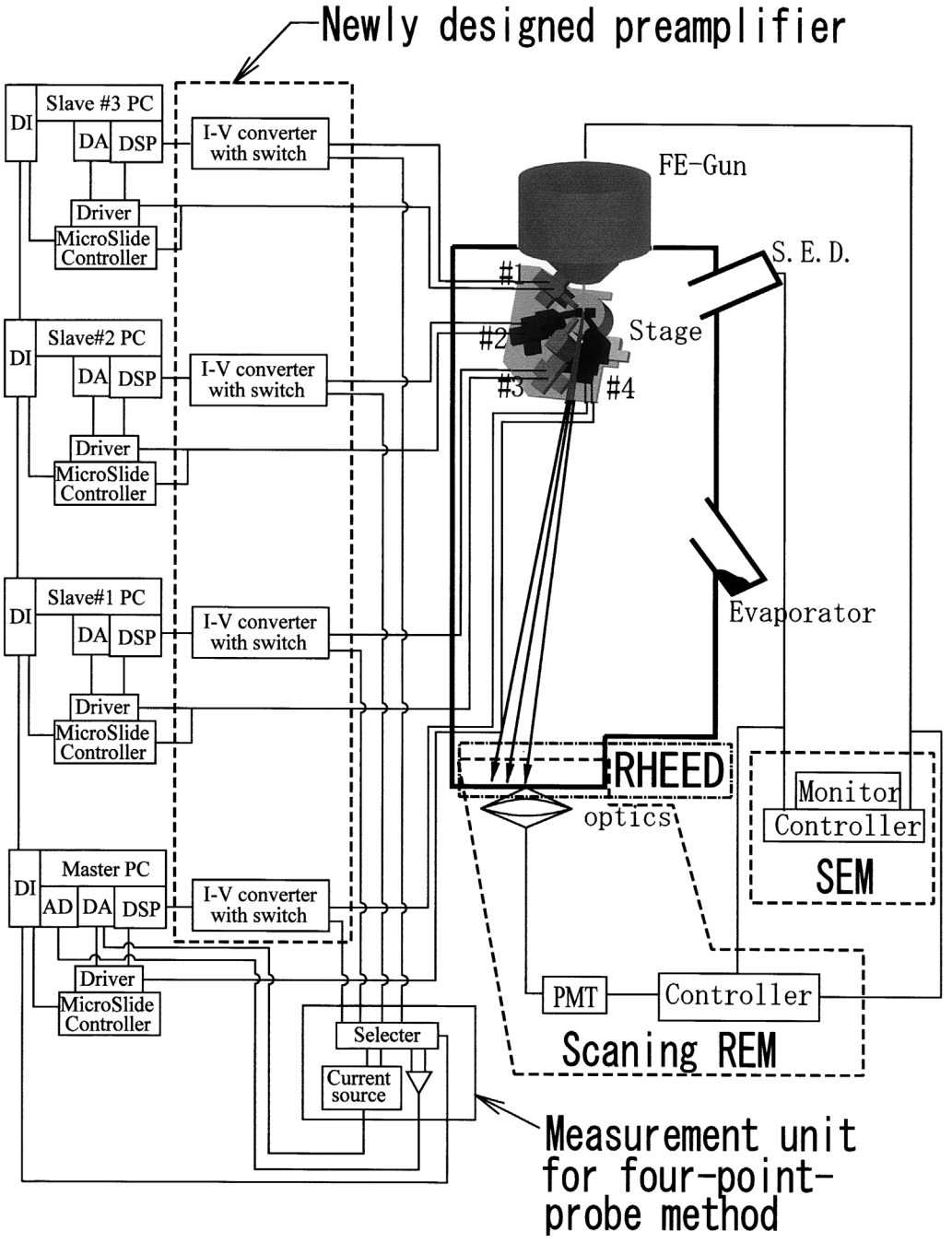

Fig. 7. A block diagram of the control system.

a few μm spacing. And then, by using the tube scanners, all of the four probes could be brought together as close as less than 1 μm easily with aid of SEM, as shown in Fig. 8(d). The minimum probe spacing attained was about 600 nm at the moment, which was determined mainly by the radii of the tip

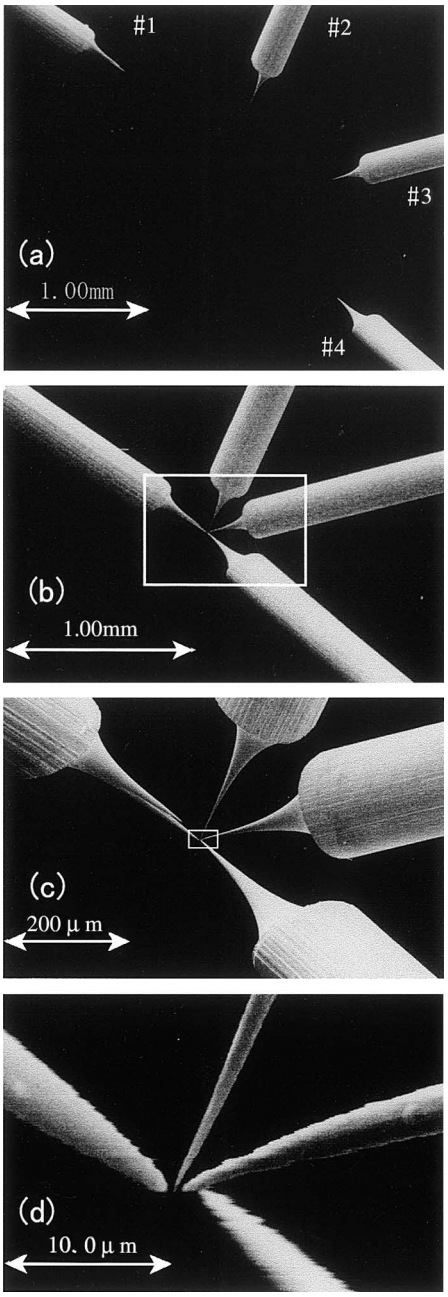

Fig. 8. SEM images for demonstrating probe positioning. (a) Initial positions of probes with spacing of ~1 mm. (b) Probes are brought close to each other by Microslides and the tube piezoelectric scanners. (c) A magnified image of the rectangular area drawn with white lines in (b). (d) A magnified image of the rectangular area drawn with white lines in (c). All of the four probes can be brought as close as less than 1 μm.

apexes. This value will be able to be improved further soon. The noise seen in Fig. 8(d) originates at the SEM imaging. After achieving such fine positioning in parallel to the sample surface, each probe was made to approach to the sample to make direct contacts to its surface. The four probes could be arranged in a line or in a square on the sample with different probe spacing with aid of in situ SEM observation.

4. Resistance measurements

By a linear four-point probe method with this apparatus in which the four tips were aligned in a line equidistantly each other on the sample surface, we measured the electrical resistance of a silicon crystal (n-type, resistivity of 5–15 Ωcm, $4 \times 15 \times 0.4$ mm^3 in size), having a Si(1 1 1)-7×7 clean surface on the front face, at room temperature in UHV. The 7×7 surface superstructure was prepared by a usual method with flash heating up to ~1250°C. Differential resistance R was measured as a gradient of I–V curve $\mathrm{d}V/\mathrm{d}I$, where V was the voltage drop measured by the inner two probes and I was the current fed through the outer probes. The current was scanned in a range e.g., between −1 and 1 μA.

Fig. 9 shows the resistances thus measured as a function of the probe spacing ranging from 1 mm to 1 μm. It is clearly shown that the resistance depends on the probe spacing d in a characteristic way; when d is smaller than 10 μm, the resistance rises significantly by more than two orders of magnitude.

When we assume the sample crystal as a homogeneous semi-infinite material, the classical electromagnetism tells us that the resistance should change as a function of d by $R = \rho/2\pi d$, where ρ is the resistivity of the crystal. A gray straight band in Fig. 9 shows this prediction when we take the value $\rho = 5$–15 Ωcm of our sample. The experimental data points are consistent with the calculated values only at $d = 10$–100 μm, while the data deviate upward from the theory at larger d and smaller d. These features with comparison to the theory were confirmed also for silicon crystals of different bulk resistivities. Therefore we can say

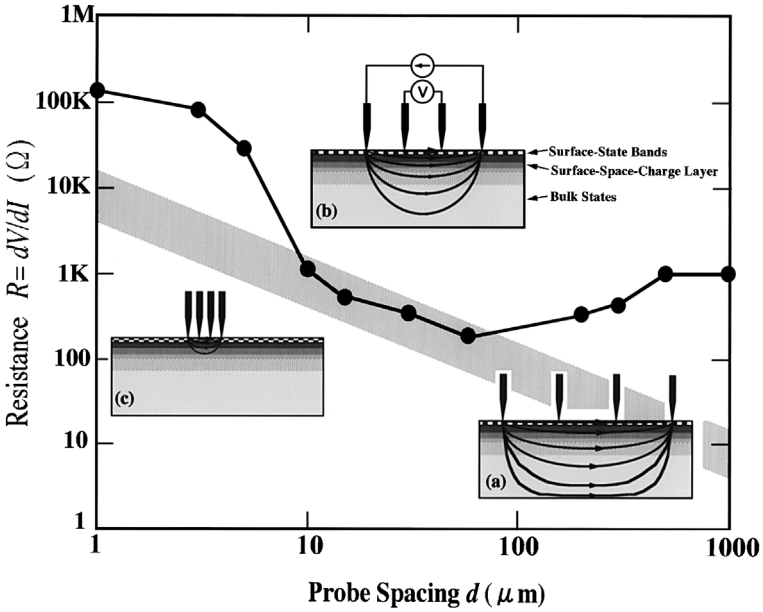

Fig. 9. Electrical resistance of a silicon crystal with a S(1 1 1)-7 × 7 clean surface on it, measured as a function of the probe spacing. Insets show schematically the current flow distribution in the sample crystal at four-point probe measurements with different probe spacings.

that our sample crystal (0.4 mm thick) can be regarded as a semi-infinite bulk when the probe spacing d is 10–100 μm, because the current distribution does not reach practically to the bottom of the crystal as schematically shown by the inset (b) in Fig. 9. When d is larger, on the other hand, the current penetrates deeper in the crystal and reach to its bottom as shown in the inset (a); the current distribution may be compressed due to the finite thickness of the sample compared with the semi-infinite case. This raises the measured resistance, which correspond to the data point at $d > 100$ μm, deviating upward from the theoretical prediction. At smaller d ranges ($d < 10$ μm), on the contrary, the current flows only near the surface as shown in the inset (c); the penetration depth of the current distribution in the sample is similar to the probe spacing in usual cases. Therefore, the data points at $d < 10$ μm in Fig. 9 indicate that the resistance near the surface is larger than that of the inner bulk region. This conclusion is reasonable when we recall a fact that the surface space-charge layer beneath the 7 × 7 clean surface is always a depletion layer, irrespective of the bulk doping concentration [7]. The width of the layer is around 1 μm for our sample, the same order as the probe spacing. Therefore, we can conclude that the resistance measurement becomes more surface-sensitive by reducing the probe spacing. The details of the quantitative analysis and results of other surface superstructures will be published elsewhere.

5. Summary

A system of independently driven four-tip probes was developed and installed in an UHV-SEM for electrical conductivity measurements by four-point probe method in nanometer regions. We designed and developed a special type of piezoelectric tube scanners for probes set out of the tube axis. A special pre-amplifier was also devised for both of STM operation with each tip and conductivity measurements with the four tips. The results of resistance measurements clearly show that we can change the measurements from bulk-

sensitive to surface-sensitive modes by reducing the probe spacing.

Acknowledgements

This work was supported in part by Grant-in-Aid from the Ministry of Education, Science, Sports, Culture of Japan, especially through those for Creative Basic Research (no. 09NP1201) conducted by Prof. K. Yagi of Tokyo Institute of Technology and also for International Joint Research (no. 11694059). We were also supported by Core Research for Evolutional Science and Technology of the Japan Science and Technology Corporation, conducted by Prof. M. Aono of Osaka University and RIKEN.

References

[1] S. Hasegawa, X. Tong, S. Takeda, N. Sato, T. Nagao, Prog. Surf. Sci. 60 (1999) 89.
[2] I. Shiraki, C.L. Petersen, P. Boggild, T.M. Hansen, T. Nagao, F. Grey, S. Hasegawa, Surf. Rev. Lett. 7 (2000) 533.
[3] C.L. Petersen, I. Shiraki, P. Boggild, T.M. Hansen, T. Nagao, F. Grey, S. Hasegawa, Appl. Phys. Lett. 77 (2000) 3782.
[4] S. Hasegawa, N. Sato, I. Shiraki, C.L. Petersen, P. Boggild, T.M. Hansen, T. Nagao, F. Grey, Jpn. J. Appl. Phys. 39 (2000) 3815.
[5] S. Hasegawa, Curr. Opin. Solid State Mater. Sci. 4 (1999) 429.
[6] M. Aono, C.-S. Jiang, T. Nakayama, T. Okuda, S. Qiao, M. Sakurai, C. Thirstrup, Z.-H. Wu, OYO BUTURI 67 (1998) 1361, in Japanese.
[7] J. Viernow, M. Henzler, W.L. O'Brien, F.K. Men, F.M. Leibsle, D.Y. Petrovykh, J.L. Lin, F.J. Himpsel, Phys. Rev. B 57 (1998) 2321.